10ème **C**ongrès **F**rançais d'**A**coustique

Lyon, 12-16 Avril 2010

Hole Interaction Effects under High and Medium Sound Intensities for Micro-Perforated Panels Design

Rostand Tayong, Philippe Leclaire

ISAT, 49 Rue Mademoiselle Bourgeois, 58027 Nevers, France rostand.tayong@u-bourgogne.fr

Most models for predicting the acoustic response of perforated panels are based on the assumption that there are no interactions between the holes. This paper investigates the Hole Interaction Effect (HIE) and distribution effect on the sound absorption coefficient of perforated panels when submitted to medium and high sound pressure levels. It is experimentally demonstrated that though the HIE is mostly an added mass effect, the nonlinear resistance parameters depend on the separation distance between the apertures. Analysis of the data reveals the fact that even with HIE, the nonlinear reactance dependency with velocity is very low compared to the resistance-velocity-dependency. Two sets of four perforated panels with hole diameters less than 2 mm with different separation distances between the holes are built and tested. Experimental results performed with an impedance tube are compared with a classical adapted model of HIE. The theoretical way of taking into account the HIE is by Fok's function. The results can be used for designing optimal perforated panels for ducts, silencers or for the automotive industry.

1 Introduction

In various noise control applications such as ducts, exhaust systems and aircraft, perforated panels are used to attenuate sound. One of the advantages of such acoustical materials is that their frequency resonances can be tuned depending on the goal to achieve. When the perforations are reduced to millimeter or submillimeter size (the term micro-perforated panel is rather used for submillimetric radius), these materials present very interesting sound absorption characteristics without any additional classical absorbing material. Moreover, they are proved to be very useful in dealing with low-frequency noise.

A large number of models have been proposed to model the acoustical behavior of perforated and micro-perforated panels. One common particularity of most of these models[1, 2, 3] is that they are only applicable for widely separated holes (assumption of no interaction between the perforations). Ingard[4] did an extensive survey on the topic of resonators. In his work, he considered the case of two apertures interacting and showed that the end-correction is highly dependent on the hole separation. The accepted study dealing with the HIE may be related to Fok[5]. From his work[5, 6], a function (called the Fok's function) was derived taking into account the distance between apertures and the correction for the radiating impedance of interacting perforations. Later, Melling[7] reconsidered this function and noted that the radiating impedance correction of Fok will be in practice small for low porosity samples ; high porosity samples will reduce the end-correction by a significant amount. Moreover, Randeberg[8] revealed specifically that the result of applying Fok's function as a correction due to the hole correction is practically equivalent to using Ingard's inner end correction for both apertures of holes in a perforated panel. If the latter studies were focused on the case of low sound intensities, there is a great need for studies dealing specifically with HIE and distribution effects under high sound intensities and the phenomena involved.

The objective of this paper is to investigate the HIE and distribution effect on the sound absorption of perforated and micro-perforated panels when backed by an air cavity under medium and high sound pressure levels. The study is focused on the case where there is no mean flow. As a first step, a function accounting for the hole interactions is derived assuming that the radiation from the aperture is spherical. Next, Ingard's classical model is described and adapted for high sound excitation with the use of high sound coefficients determined by a fitting technique. The experimental setup is then described. The measurements are carried out on two sets of plates (one set focused on the hole interactions only and the other focused on the distribution and the interaction effects) with different separations between the holes (from widely separated to closely separated holes). The effect of hole interaction on the resistance and the reactance is particularly discussed. The other important results are summarized in the conclusion of this paper.

2 Theoretical formulations

2.1 Hole interaction function : Fok's function

In this study, the radiation of sound from the aperture is considered to be spherical. Assuming equal radiation in all directions, the wave equation in one di-

mensional spherical coordinates is written as

$$\frac{\partial^2 p}{\partial r^2} + \frac{2}{r}\frac{\partial p}{\partial r} = \frac{1}{c_0^2}\frac{\partial^2 p}{\partial t^2}, \tag{1}$$

where p is the sound pressure and c_0 is the sound velocity in air. Under the latter assumption, the sound wave will expand as it travels away from a single aperture and the wave front remains a spherical surface. At the outlet of the aperture, the flow field can be studied in terms of pressure, velocity or even shear. Considering the case of 2 apertures interacting, Ingard[4] found that the end-correction is very dependent on the holes separation and that the interaction impedance can be determined from

$$z_{1,2} = \frac{1}{U_2 S_2}\int_{S_2} p_{1,2} dS_2, \tag{2}$$

where $p_{1,2}$ is the pressure exerted by hole 1 at hole 2, U_2 is the volume velocity through hole 2 and S_2 is the area of hole 2. Determining $z_{1,2}$ would lead to a new end-correction factor and therefore to a new specific impedance expression. Solving equation (2) for the case of infinitely thin plates, Fok's work[5, 6] provides an expression for an attached conductance and for a function of variable d/b expressed as

$$\psi(\xi) = 1 + x_1\xi + x_2\xi^2 + x_3\xi^3 + x_4\xi^4 + x_5\xi^5 + x_6\xi^6 + x_7\xi^7 + x_8\xi^8, \tag{3}$$

where $\psi(\xi)$ is the so-called Fok function of variable d/b. With $x_1 = -1.4092$; $x_2 = 0$; $x_3 = +0.33818$; $x_4 = 0$; $x_5 = +0.06793$; $x_6 = -0.02287$; $x_7 = +0.03015$; $x_8 = -0.01641$, and d is the hole diameter.

It is shown from fig.6 of Ref. [7] that if $d/b < 0.2$, there is no appreciable interaction effect and that if $d/b > 0.8$, the attached mass is effectively zero.

2.2 Surface impedance and absorption coefficient accounting for the holes interactions effects

To take into account the interaction effects of apertures, Rschevkin[6] proposed modifying the end-correction term of the perforated panel model with the Fok's function. Due to flow of air through the holes which affects the air close to the inner and outer apertures, the thickness must be corrected with an additional term[1]. For circular cross-section holes, Rayleigh[9] proposed an end correction δ for the inner and outer aperture as follows

$$\delta = \frac{8d}{3\pi}, \tag{4}$$

where d is the hole diameter. Following Ingard's work[4, 8], the specific acoustic impedance of a single aperture taking into account the inner and outer aperture is given by

$$Z_1 = 4R_s(1 + \frac{h}{d}) + j\omega\rho_0(h + \delta), \tag{5}$$

where h is the panel thickness, ρ_0 is the density of air, ω is the radian frequency and R_s is the surface resistance due to the viscous dissipation in the aperture and the surface of the panel given by

$$R_s = \frac{1}{2}\sqrt{2\omega\rho_0\mu}, \tag{6}$$

where μ is the coefficient of viscosity of air. Finally, the total specific impedance Z_p of the perforated panel with interacting holes is given by

$$Z_p = \frac{4R_s}{\sigma}(1 + \frac{h}{d}) + \frac{j\omega\rho_0}{\sigma}(h + \frac{\delta}{\psi(\xi)}), \tag{7}$$

where σ is the open area ratio and $\psi(\xi)$ the Fok's function as described in the above section. According to Ingard[4], under high sound intensities, assuming that the reactance dependence on velocity is negligible, the resistance velocity-dependent expression is given by

$$\frac{R_{nl}}{d} = K_1\left(\frac{U}{100}\right)^{C_2}, \tag{8}$$

where R_{nl} is the nonlinear resistance, U is the average incident velocity, K_1 and C_2 are constants that may depend on frequency. For a single frequency and using the Reynolds number, expression (8) can be transformed into

$$R_{nl} = C_1 \mathrm{Re}^{C_2}, \tag{9}$$

where Re is the Reynolds number, C_1 and C_2 are the nonlinear resistance coefficients determined experimentally. These coefficients lead to the best fit of the nonlinear resistance curves. Their values for the samples used for measurements are given in Table 2. The Reynolds number is expressed as

$$\mathrm{Re} = \frac{dU}{\nu}, \tag{10}$$

with ν the kinematic viscosity. If the perforated panel is backed by an air cavity, the resonant system formed has an impedance given by

$$Z_s = Z_p + Z_{cav}, \tag{11}$$

where Z_{cav} is the air cavity impedance expressed as

$$Z_{cav} = -jZ_0\cot(k_0 D_c), \tag{12}$$

Z_0 being the impedance of air, k_0 is the wave number and D_c the air cavity depth. The reflection coefficient is obtained using the formula

$$R = \frac{Z_s - Z_0}{Z_s + Z_0}, \tag{13}$$

and the absorption coefficient is given as

$$\alpha = 1 - |R|^2. \tag{14}$$

3 Experimental setup and results discussion

All the measurements are performed on steel perforated panels. Each panel sample has an external diameter of 100 mm. The mounting conditions of the samples inside the tube are close to a clamped condition. Pictures of the two sets of samples used in the experiments are shown in Figs. 1 and 2 and the samples characteristics are given in Table 1. A schematic of the impedance tube used for the experiments is shown in Fig. 3. It is a rigid circular plane-wave tube with a diameter of 100

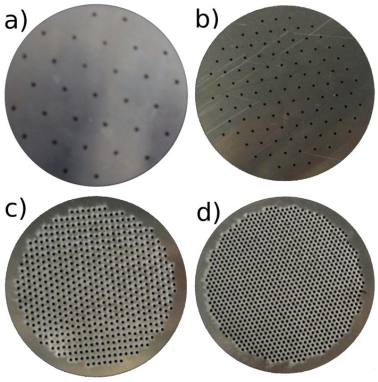

FIG. 1 – Sample pictures of group A set (for the holes interactions effect). a) sample 1A ; b) sample 2A ; c)sample 3A ; d) sample 4A.

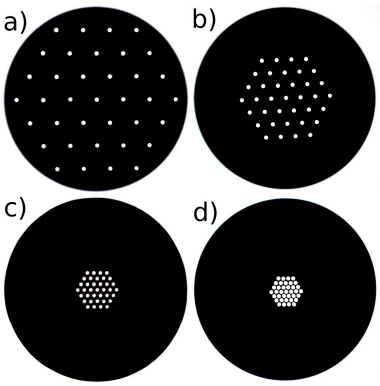

FIG. 2 – Sample pictures of group B set (for the holes distribution effect). a) sample 1B ; b) sample 2B ; c)sample 3B ; d) sample 4B.

mm (cut-off frequency of 1.7 KHz). On the left hand side, a JBL model compression driver is mounted as the excitation source. This compression driver is powered by a power amplifier. A transition piece provides the continuity transition between the circular section of the compression driver and the circular cross section of the impedance tube. On the right hand side of the tube, a soundproof plunger is used as the rigid backing wall. The sealing for the plunger is ensured using a rubber seal. By moving the plunger along the longitudinal axis of the tube, it is possible to create an air cavity behind the sample. Three $1/4''$ microphones are used to perform the signal detection. The first two microphones (micro 1 and 2 in Fig. 3) are used to calculate the surface impedance of the sample by the two-microphone standing waves method described by Chung and Blaser[10]. The distance between these microphones is s = 50 mm. And the distance between microphone 2 and the sample is about $l_2 = 11$ mm. The third microphone (reference micro in Fig. 3) is used to monitor the level of pressure at the sample surface. The measurements are performed taking a single sample panel with an air cavity depth behind and a rigid wall.

3.1 Hole interactions effects and the nonlinear resistance

Figure 4 shows the normalized surface resistance of group A samples as a function of the Reynolds number in

	h(mm)	d(mm)	b(mm)	σ(%)
Sample 1A	1.5	1.6	12	1.92
Sample 2A	1.5	1.6	8.0	4.25
Sample 3A	1.5	1.6	3.5	20.52
Sample 4A	1.5	1.6	2.6	35.28
Sample 1B	2.0	1.6	14.18	0.95
Sample 2B	2.0	1.6	8.0	0.95
Sample 3B	2.0	1.6	3.5	0.95
Sample 4B	2.0	1.6	2.6	0.95

TAB. 1 – Dimensions of the perforated samples.

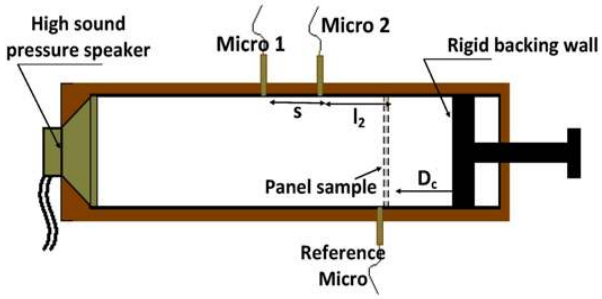

FIG. 3 – Schematic of the impedance tube used for the measurements.

front of the apertures. The symbols represent the experimental results whereas the lines (continuous, dashed, dot-dashed) and dots represent the power fitting curve as expression (9). The resulting fitting coefficients are given in Table 2. The second coefficient C_2 is found to be around a value of 1, therefore confirming similar observations from Ref.[4, 7] where it is proved that for high sound excitation levels, the dependency of the resistance with the velocity is linear. The first coefficient C_1 can then be considered as the slope. It is observed in Fig. 4 that this slope decreases with the decrease of the pitch distance b between the holes. From this result, it is clear that for high sound excitations, this slope depends on the hole separation. For very close holes (samples 3A and 4A for instance), this slope tends to zero. Therefore the hole interaction effect decreases the nonlinear resistance. A convenient explanation of this observation is that as the pitch distance b between the holes decreases, the shear region around each hole is shared with the shear region around the nearby holes. Since the total shear region is reduced with interacting holes, this causes a reduction of the radiation resistance. The reduction of this end correction resistance results in a reduction of the surface resistance.

	C_1	C_2
Sample 1A	0.241	1.05
Sample 2A	0.049	0.98
Sample 3A	0.004	0.99
Sample 4A	0.003	0.99

TAB. 2 – Curve fitting constants for the nonlinear resistance of group A samples.

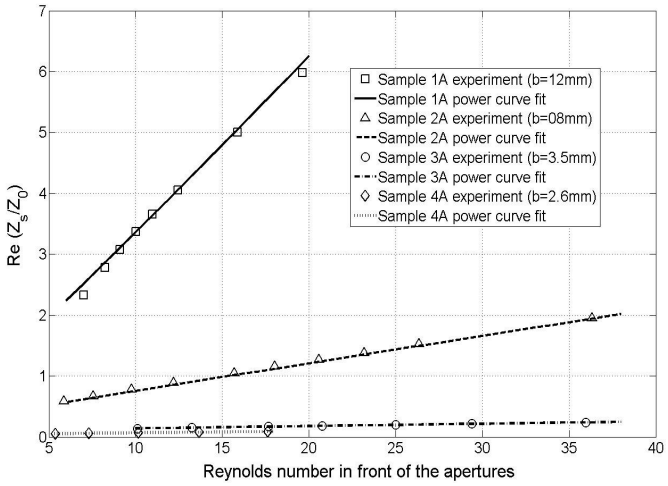

FIG. 4 – Normalized surface resistance as a function of the Reynolds number in front of the apertures for group A samples. Excitation frequency of 506 Hz.

3.2 Hole interactions effects and the nonlinear reactance

Figure 5 shows the experimental results of the normalized surface reactance as a function of the Reynolds number in front of the apertures for group A samples (for 506 Hz). As it was already noted by Melling[7], with the increase of sound excitation levels, the reactance decreases. This is typical nonlinear behavior of the reactance of thin plates whenever turbulence is reached (see Ref.[4]). This decrease is caused by a transfer of part of the kinetic energy in the sound field around the aperture into turbulent motion that breaks away from the aperture. Since this behavior is less likely for the cases of closely separated holes (samples 3A and 4A), it is observed that with the decrease of the pitch distance b between the holes, the reactance decreases less. A physical meaning of this last observation would be that the closer the holes are to each other, the less particles are blown out from around the aperture.

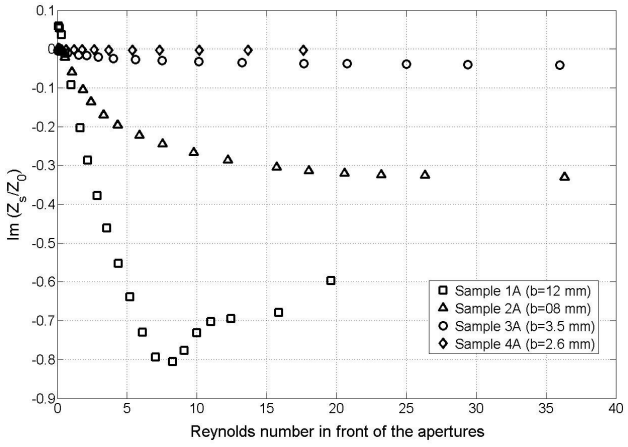

FIG. 5 – Experimental results of the normalized surface reactance as a function of the Reynolds number in front of the apertures for group A samples. Excitation frequency of 506 Hz.

3.3 Hole interactions effects and the absorption coefficient

Figure 6 shows the experimental and simulated results of the absorption coefficient at the resonant frequency of 506 Hz for group A samples as a function of the Reynolds number in front of the apertures. The simulations and the experiments are in very good agreement. Depending on the sample characteristics (hole diameters and open area ratio), with the increase of Reynolds number, the maximum absorption is shown (Ref.[11]) to rise to a maximum value of 1 in a first phase and then decrease in a second phase. The critical Reynolds number is obtained at the point at which the latter phases change. This is verified for sample 2A and would take place beyond the Reynolds number range of study for samples 3A and 4A. Therefore, if the pitch distance b between the holes is optimized, the HIE can contribute interesting absorption coefficient increase under medium and high sound intensities.

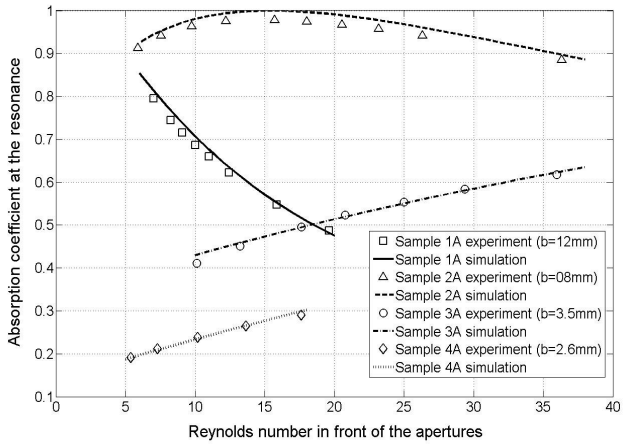

FIG. 6 – Absorption coefficient at the resonance as a function of the Reynolds number in front of the apertures for group A samples. Excitation frequency of 506 Hz.

3.4 Experimental results of the holes distribution effects on the absorption coefficient

Figure 7 shows the experimental results of the absorption coefficient as a function of frequency at 100 dB and 140 dB for the group B samples. In this sample group, the global open area ratio is 0.95% for all the samples with different pitch distance b between the holes. The holes are therefore not regularly distributed over the entire plate surface. It is observed that in both cases, this distribution effect is rather much an added mass effect since it mainly displaces the resonant frequency. A decrease of the pitch distance b between the holes with the same open area ratio results in shifting the resonant frequency towards the low frequency ranges.

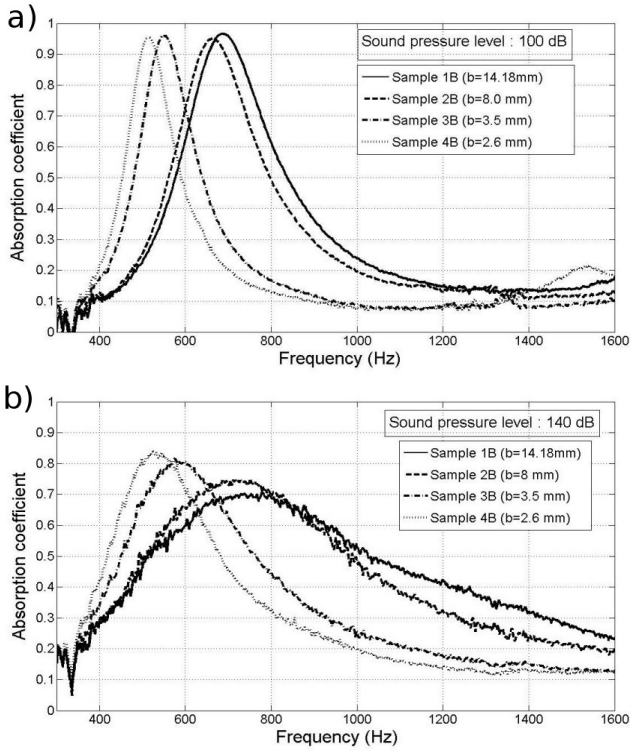

FIG. 7 – Experimental results of the absorption coefficient of the samples of group B as a function of the frequency. for a) 100 dB ; b) 140 dB. Focus on the distribution effect.

4 Conclusion

An investigation of the Hole Interaction Effects (HIE) of air-cavity-backed perforated panels under high and meduim sound intensity levels was carried out in this paper. It was demonstrated experimentally that the nonlinear resistance slope directly depends on the separation distance between the holes. It was also demonstrated that even with HIE, the nonlinear reactance is even less dependent of the incident Reynolds number. It was also seen that the interaction effect can improve the absorption coefficient amplitude of the perforated panel system for medium and high sound levels for optimized distance between the holes. This interaction effect can be used to increase the critical point after which the absorption coefficient starts to decrease with the increase of sound intensity. With this shift of the critical point, a certain compromise may be made between the low, medium and high intensity absorptions results. Nevertheless, this critical point definitely depends also on the aperture pitch distance. This study was done only for the case of normal incident waves, and it would be interesting to look into these interaction effects when submitted to bias or grazing flow under high levels of excitation. Further theoretical investigations are also needed to explain the behavior of the jet formation with the HIE.

Références

[1] Allard J.F., "Propagation of sound in porous media. Modelling sound absorbing materials", Elsevier, London, (1993)

[2] Maa D.Y., "Potential of Micro-perforated panel absorber", *J. Acoust. Soc. Am.* 104, 2861-2866 (1998)

[3] Hersh A.S., Walker B.E., Celano J.W., "Helmholtz Resonator Impedance Model, Part I :Nonlinear Behavior", *Am. Inst. Aeron. Astron.* 41 (5), 795-808 (2003)

[4] Ingard U., "On the Theory and Design of Acoustic Resonators", *J. Acoust. Soc. Am.* 25 (6), 1037-1061 (1953)

[5] Fok V.A., "Doklady akademii nauk", *SSSR* 31, (1941)

[6] Rzhevkin S.N., "A Course of Lectures on the Theory of Sound", Pergamon Press, London, (1963)

[7] Melling T.H., "The acoustic Impedance of perforates at medium and high sound pressure levels", *J. Sound Vib.* 29 (1), 9-12 (1973)

[8] Randeberg R.T., "Perforated Panel Absorbers with Viscous Energy Dissipation Enhanced by Orifice Design", PhD Thesis, Trondheim, 15-18, (2000)

[9] Rayleigh L., "Theory of sound II.", Macmillan, London, (1940)

[10] Chung J.Y., Blaser D.A., "Transfer function method of measuring in-duct acoustic properties. Part I Theory", *J. Acoust. Soc. Am.* 68 (3), 907-913 (1980)

[11] Tayong R., Dupont T., Galland M.A., Leclaire P. "High sound pressure models for microperforated panels backed by an air cavity", *in Proc. ASA* 155^{th} *meeting*, Paris (2008)